scientific reports

Check for updates

OPEN

Hinokiflavone is a novel CK2 inhibitor promoting apoptosis and synergizing with chemotherapeutic agents in cisplatin resistant bladder cancer cells

Tsung-Han Hsieh[1,10], Han-Pin Kuo[2,3,10], Mei-Chuan Chen[4], Yu-Chen Lin[5,6], Bo-Jyun Lin[5,6], Kai-Cheng Hsu[7,8] & Chun-Han Chen[5,6,9]✉

Bladder cancer (BC) remains a major therapeutic challenge, particularly in patients with acquired resistance to platinum-based chemotherapy. In this study, we investigated the potential of hinokiflavone (HNK), a natural biflavonoid, as a therapeutic agent against cisplatin-resistant BC. Our results demonstrate that HNK differentially inhibited the proliferation of cisplatin-resistant BC cells while sparing normal uroepithelial cells. Mechanistically, HNK induced apoptosis through both intrinsic and extrinsic pathways, as evidenced by caspase activation and Annexin V staining. Next-generation sequencing and gene set enrichment analysis revealed that HNK modulates genes involved in biosynthesis, metabolism, DNA replication and DNA repair. Additionally, HNK downregulated the transcription of *MUTYH*, *OGG1*, and *XRCC1*, which are key genes in base excision repair. For the first time, we identified that HNK as a novel inhibitor of CK2α via in vitro kinase assays, substrate phosphorylation assays, and molecular docking analysis. HNK treatment reduced the phosphorylation of known CK2α targets, including Akt, Stat3, and XRCC1, in cisplatin-resistant BC cells. Time-course analysis revealed that the inhibition of Akt phosphorylation coincided with PARP cleavage, and genetic rescue experiments confirmed the involvement of the CK2α/Akt axis in HNK-induced apoptosis. Furthermore, combination treatment with HNK and chemotherapeutic agents such as doxorubicin or mitomycin C resulted in enhanced cytotoxic effects, suggesting a potential role of HNK as a chemosensitizing agent. HNK, by targeting both DNA repair pathways and CK2-mediated survival signaling, may serve as a promising therapeutic candidate for cisplatin-resistant BC.

Keywords Bladder cancer, Cisplatin, CK2, Apoptosis

Bladder cancer (BC) is the most common malignancy of the urinary tract worldwide, with an estimated 613,791 new cases and 220,349 deaths annually[1]. Unfortunately, BC is characterized by high recurrence rates, tumor heterogeneity, and resistance to platinum-based therapy, leading to a significant burden on health care systems and negatively impacting patient outcomes[2]. Approximately 80% of patients are initially diagnosed with non-muscle invasive BC (NMIBC), 50–70% of whom experience disease recurrence and 10–15% of whom progress to muscle-invasive bladder cancer (MIBC)[3]. Patients with MIBC have a reported 5-year survival rate of 40–60%, which drastically decreases to 6% once the disease progresses to the metastatic stage[4]. Platinum-based

[1]Precision Health Center, Taipei Medical University, Taipei 110301, Taiwan. [2]Center of Thoracic Medicine, Taipei Medical University, Taipei 110301, Taiwan. [3]Department of Thoracic Medicine, Taipei Medical University Hospital, Taipei 110301, Taiwan. [4]School of Pharmacy, College of Pharmacy, Taipei Medical University, Taipei 110301, Taiwan. [5]Graduate Institute of Medical Sciences, College of Medicine, Taipei Medical University, Taipei 110301, Taiwan. [6]Department of Pharmacology, School of Medicine, College of Medicine, Taipei Medical University, Taipei 110301, Taiwan. [7]Graduate Institute of Cancer Biology and Drug Discovery, College of Medical Science and Technology, Taipei Medical University, Taipei 110301, Taiwan. [8]Ph.D. Program for Cancer Molecular Biology and Drug Discovery, College of Medical Science and Technology, Taipei Medical University, Taipei 110301, Taiwan. [9]Cell Physiology and Molecular Image Research Center, Wan Fang Hospital, Taipei Medical University, Taipei 116079, Taiwan. [10]These authors contributed equally: Tsung-Han Hsieh and Han-Pin Kuo. ✉email: brianchc@tmu.edu.tw

chemotherapy followed by radical cystectomy is the current standard of care for MIBC patients[4], however, its efficacy is limited by a high recurrence rate, and many patients are ineligible for this treatment owing to poor renal function or comorbidities[5,6]. Although immune checkpoint inhibitors (ICIs), such as PD-1 inhibitors (e.g., pembrolizumab and nivolumab) and PD-L1 inhibitors (e.g., atezolizumab), have demonstrated clinical benefits in advanced BC patients[7], the overall response rate remains low (only 15–25%), and primary or acquired resistance continues to present a significant challenge[8]. Novel approaches targeting frequent genetic alterations in advanced BC are currently under investigation and have led to the approval of targeted therapies such as FGFR inhibitors (e.g., erdafitinib)[9]. In 2023, the US FDA approved the combination of enfortumab vedotin and pembrolizumab, which, compared with chemotherapy, prolonged the progression-free survival (PFS) and overall survival (OS) of patients with previously untreated locally advanced or metastatic BC[10]. However, 55.9% of BC patients experienced grade 3 or higher treatment-related adverse events[11]. Therefore, the lack of an effective non-platinum-based neoadjuvant treatment remains a significant barrier to improving BC patient outcomes.

Platinum-based drugs have been used for the treatment of solid malignancies, and the most common regimens for BC are methotrexate, vinblastine, doxorubicin, and cisplatin (MVAC), dose-dense MVAC (ddMVAC), and gemcitabine plus cisplatin (GC)[6]. The overall survival of most patients receiving cisplatin-based chemotherapy ranges from 9 to 15 months, and for those with disease relapse after platinum-based chemotherapy, the median survival is further reduced to 5 to 7 months[12]. Upon entering a cell, cisplatin is activated through the replacement of its two chloride ligands with water molecules, allowing it to react with the N7 atoms of purine bases and form various DNA adducts. The resulting DNA lesions subsequently trigger the DNA damage response and induce mitochondrial apoptosis[13]. However, cisplatin treatment often leads to the development of chemoresistance, ultimately resulting in therapeutic failure in BC. Several mechanisms contribute to cisplatin resistance, including reduced intracellular drug bioavailability due to decreased influx, increased efflux, and intracellular sequestration, as well as enhanced DNA repair mechanisms or an attenuated apoptotic cascade[14]. As platinum-based chemotherapy remains the primary therapeutic option for patients with advanced BC, developing chemosensitizing strategies is crucial for improving clinical outcomes.

Natural products (NPs) derived from living organisms such as plants, animals, and microbes have historically played pivotal roles in treating human diseases[15]. Notably, nearly half of all anticancer drugs approved between 1981 and 2019 originated from NPs, underscoring the significant contribution of NPs to drug discovery and cancer treatment[16]. Several chemotherapeutic agents derived from NPs, including paclitaxel, docetaxel, doxorubicin, vinblastine, and mitomycin C, are routinely used to treat BC[17]. Enfortumab vedotin, an antibody–drug conjugate that targets nectin-4 and is linked to the microtubule-disrupting agent monomethyl auristatin E (MMAE), a synthetic analog of marine-derived compound, received FDA approval in 2019 for the treatment of advanced BC[18]. Those findings and approvals highlight the continued importance of NPs as valuable resources for drug discovery. Flavonoids represent the largest group of polyphenolic compounds found in nature[19]. Numerous studies have reported that flavonoids act as antioxidants, playing crucial roles in scavenging reactive oxygen species (ROS), triggering apoptotic pathways, and inhibiting inflammatory signaling pathways[20]. Biflavonoids are composed of two phenyl-chromenone units linked via C–C or C–O–C bonds, forming dimeric flavonoids[21]. Hinokiflavone (HNK), a bis-apigenyl ether, was first isolated from the dried leaves of *Chamaecyparis obtusa* Endlicher in 1958 in Japan[22], it can be synthesized and has also been identified in various plant species within the *Cupressaceae* and *Taxaceae* families[23–25]. Previous studies on the pharmacological profile of HNK have demonstrated its anti-inflammatory, antioxidant, and antitumor activities[26–29]. In addition to exhibiting potent antiproliferative and antimigratory effects in vitro, HNK has shown in vivo antitumor activity against breast cancer, colon cancer, and hepatocellular carcinoma (HCC)[29–31]. However, its potency and mechanisms of action against platinum-resistant BC remain unknown, necessitating further research to support and optimize its clinical applicability in BC.

In this study, we observed that HNK had antiproliferative effects and promoted the apoptosis of cisplatin-resistant BC cells. Mechanistically, HNK inhibited CK2α activity, leading to the reduced phosphorylation of key proteins involved in survival signaling (Akt, Stat3) and DNA repair (XRCC1). HNK also downregulated the expression of base excision repair genes, including *MUTYH*, *OGG1*, and *XRCC1*. The inhibition of Akt dephosphorylation was temporally associated with PARP cleavage, and genetic rescue experiments confirmed the involvement of the CK2α/Akt axis in HNK-induced apoptosis. Additionally, HNK enhanced the cytotoxic effects of chemotherapeutic agents such as doxorubicin and mitomycin C. Collectively, HNK targets both survival and DNA repair pathways, supporting its potential as a therapeutic and chemosensitizing agent in cisplatin-resistant BC.

Materials and methods

Cell culture and reagents

NTUB1 and N/P(14) (a cisplatin-resistant subline) cells were obtained from Dr. Tzyh-Chyuan Hour (Kaohsiung Medical University) and cultured as previously described[32,33]. J82 and SV-HUC-1 cells were purchased from American Type Culture Collection (Manassas, VA, USA). The cisplatin-resistant subline of J82 (J82R) cells was generated by gradually increasing the cisplatin concentration until the cells adapted to 10 μM. All cell lines were maintained at a passage number below 10, and mycoplasma contamination was routinely tested by PCR analysis. Cells were cultured in RPMI 1640 (NTUB1, N/P(14)), EMEM (J82), or F12K (SV-HUC-1) growth media at 37 °C with 5% CO_2, supplemented with 10% FBS and 1X antibiotic-antimycotic (Thermo Fisher Scientific, Waltham, MA, USA). Hinokiflavone (HY-N2360) and CX-4945 (HY-50855) were purchased from MedChem Express (Monmouth Junction, NJ, USA). Cisplatin (13119), doxorubicin (15007), and mitomycin C (11435) were obtained from Cayman Chemicals (Ann Arbor, MI, USA). All other chemicals used in this study were purchased from Sigma-Aldrich (St. Louis, MO, USA).

Sulforhodamine B (SRB) assay

Cells were seeded into 96-well plates and treated with hinokiflavone for 48 h. After treatment, the cells were fixed with 10% TCA, stained with 0.4% SRB dye, washed with 1% acetic acid, and solubilized in 10 mM Tris base. Absorbance at 515 nm was measured using a spectrophotometer, and the drug concentration required to achieve 50% inhibition of cell growth (GI_{50}) was calculated as previously described[34]. The combination index (CI) values were determined using CompuSyn 1.0.1 software (ComboSyn, Inc., Paramus, NJ, USA; www.combosyn.com), where a CI value below one indicates synergism.

Flow cytometry analysis

Cells were seeded in 6-well plates and treated with hinokiflavone. After treatment, the cells were trypsinized, washed with PBS, fixed at −20 °C with 75% ethanol, and stained with propidium iodide (80 µg/mL) containing 0.1% Triton X-100 and RNase A (100 µg/mL) for cell cycle analysis, as previously described[34]. For apoptosis detection, cells were collected and stained with the Muse Annexin V & Dead Cell Kit (Luminex, Austin, TX, USA) for 20 min. The samples were then analyzed using the Guava Muse Cell Analyzer (Luminex), as previously described[35].

Western blot analysis and transient transfection

Cells were treated with the indicated compounds, and proteins were extracted using SDS lysis buffer. The extracted proteins were separated by SDS-PAGE, transferred onto a polyvinylidene difluoride (PVDF) membrane, and analyzed as previously described[34]. The antibodies used in this study were obtained from the following sources: PARP (CS9542), caspase-8 (CS9746), caspase-9 (CS9502), phospho-CK2 Substrate [(pS/pT)DXE] (CS9738), Akt (CS9272), Phospho-Stat3 (Tyr705) (CS9145), Stat3 (CS9139) and XRCC1 (CS76998) were obtained from Cell Signaling Technology (Danvers, MA, USA); MUTYH (19650-1-AP) and OGG1 (15125-1-AP) were obtained from Proteintech (Rosemont, IL, USA); GAPDH (GTX100118) was obtained from GeneTex (Irvine, CA, USA); caspase-3 (NB100-56708) was purchased from Novus (Littleton, CO, USA); phospho-Akt (S129) (ab133458) was obtained from Abcam (Cambridge, UK); CK2α (GTX107897) and GAPDH (GTX100118) were obtained from GeneTex (Irvine, CA, USA); and phospho-XRCC1 (A300-059 A) was purchased from Thermo Fisher Scientific. The band intensities of each protein were quantified using ImageJ software (Version 1.53, National Institutes of Health; Bethesda, MD, USA; https://imagej.net/ij/). For transient overexpression, the cells were seeded in 6-well plates, and transfected with CK2α (OHu26801; GenScript, Piscataway, NJ, USA) and myristoylated Akt (Myr-Akt; Addgene, Cambridge, MA, USA) plasmids by using a TurboFect transfection reagent (Thermo Fisher Scientific) following the manufacturer's instructions.

Next-Generation sequencing (NGS) and bioinformatic analysis

N/P(14) cells were plated in 6 cm dishes and treated with hinokiflavone (5 µM) for 24 h. Cells were then collected by scraping, washed with PBS, and lysed using TRIzol reagent (Thermo Fisher Scientific) for RNA extraction. Library preparation and sequencing were performed as previously described[36]. The data generated in this study are publicly available in Gene Expression Omnibus (GEO) at GSE290747. Differentially expressed genes were identified using DESeq2 (version 1.28.0). The gene set enrichment analysis was performed by using the GSEA software (version 4.0.3) (https://www.gsea-msigdb.org/gsea/index.jsp), and the "c2.cp.kegg.v7.2.symbols.gmt" subset was used to evaluate relevant pathways[37,38]. The results were considered significant if the false discovery rate (FDR) is less than 0.25 and the absolute value of the normalized enrichment score (NES) is greater than 1.

Reverse transcription quantitative PCR

Total RNA was extracted from treated cell samples using TRIzol reagent (Thermo Fisher Scientific) according to the manufacturer's instructions. Briefly, cells were lysed with TRIzol reagent, followed by the addition of 1-bromo-3-chloropropane. After centrifugation, the aqueous phase containing RNA was collected and mixed with isopropyl alcohol to precipitate the RNA. The RNA pellet was washed with 75% ethanol and then resuspended in RNase-free water and reverse transcribed into complementary DNA using the HiScript™ I First Strand cDNA Synthesis Kit (Bionovas, Toronto, ON, Canada). Quantitative PCR was then performed using gene-specific primers (Supplementary Table S1) and the RealQ Plus 2X Master Mix Green Kit (Ampliqon, Odense, Denmark), as previously described[35].

In vitro CK2α kinase activity assay.

The inhibitory activity of hinokiflavone on CK2α was assessed using the services of Reaction Biology Corp (Malvern, PA, USA). The compound was tested in a 10-dose format with a threefold serial dilution starting at 100 µM in the presence of 10 µM ATP. The data were presented as the percentage of kinase activity relative to the control group.

Molecular docking

Molecular docking analysis was carried out using Maestro with standard settings[39]. The crystal structure of CK2 alpha (PDB ID: 8QWY) was downloaded from the RCSB Protein Data Bank (PDB)[40]. The structure was first prepared using the Protein Preparation Wizard, which included the addition of hydrogen atoms, assignment of partial charges, and removal of water molecules. A receptor grid was generated using the Receptor Grid Generation module, centered on the co-crystallized ligand. The compound was prepared using the LigPrep module. Subsequently, the compound was docked into the binding site of CK2 alpha using GLIDE[41]. After docking, interactions between the compound and protein residues were analyzed using Pipeline Pilot Client 2021 (https://www.3ds.com/products/biovia/pipeline-pilot)[42].

Statistical analysis

Data analysis was performed using GraphPad Prism software (10.4.1) (GraphPad Software, Boston, Massachusetts, USA; www.graphpad.com). Statistical comparisons between two groups were conducted using two-tailed Student's *t*-test. One-way or two-way analysis of variance (ANOVA) with post-hoc analysis were used for comparisons among multiple groups. Details on group sizes and statistical methods are provided in the figure legends. A *p*-value of less than 0.05 was considered statistically significant.

Results

HNK exhibits stronger antiproliferative effects on cisplatin-resistant BC cells than on normal uroepithelial cells

To evaluate the anticancer activity of HNK in cisplatin-resistant BC, NTUB1 cells (a high-grade urothelial carcinoma cell line) and its corresponding cisplatin-resistant subline, N/P(14) cells, were used as representative models for cisplatin-sensitive and cisplatin-resistant BC cells, respectively[33]. Additionally, cisplatin-resistant J82 (J82R) cells were generated by gradually exposing parental J82 cells to increasing concentrations of cisplatin. The results demonstrated that both N/P(14) and J82R cells exhibited significant resistance to cisplatin, as confirmed by the SRB assay (Fig. 1a and b). The GI_{50} values for cisplatin were 7.89 μM and 47.4 μM in NTUB1 cells and N/P(14) cells, respectively. and 2.58 μM and 9.47 μM in J82 cells and J82R cells, respectively. HNK (Fig. 1c) displayed selective anti-proliferative activity, inhibiting the growth of N/P(14) and J82R cells more effectively than that of normal uroepithelial SV-HUC-1 cells, with GI_{50} values of 1.48 μM, 0.98 μM and 4.09 μM, respectively (Fig. 1d). In summary, our findings indicate that HNK significantly inhibits the growth of cisplatin-resistant BC cells while sparing normal uroepithelial cells.

HNK induces apoptosis in cisplatin-resistant BC cells

To elucidate the mechanism underlying HNK-induced antiproliferative activity, we examined the effect of HNK on cell cycle progression using PI staining and flow cytometry. HNK significantly increased the accumulation of cells in the sub-G1 phase in a time- and concentration-dependent manner (Fig. 2a and b). Annexin V/7-AAD double staining further revealed a significant increase in the percentage of early- and late-apoptotic N/P(14) cells treated with HNK (Fig. 2c and d), indicating that apoptosis was induced. Consistent with these findings, HNK treatment also significantly increased the sub-G1 population and number of apoptotic J82R cells (Supplementary Figs. S1a and S1b). Moreover, HNK enhanced the cleavage of caspase-3, caspase-8, caspase-9, and PARP in both N/P(14) and J82R cells (Fig. 3a and b). These results suggest that HNK induces both intrinsic and extrinsic apoptosis in cisplatin-resistant BC cells.

Differentially expressed genes (DSGs) affected by HNK in N/P(14) cells

To elucidate the mechanisms underlying HNK-induced apoptosis, next-generation sequencing (NGS) was performed to characterize the differentially expressed genes (DEGs) in N/P(14) cells. The cells were treated with

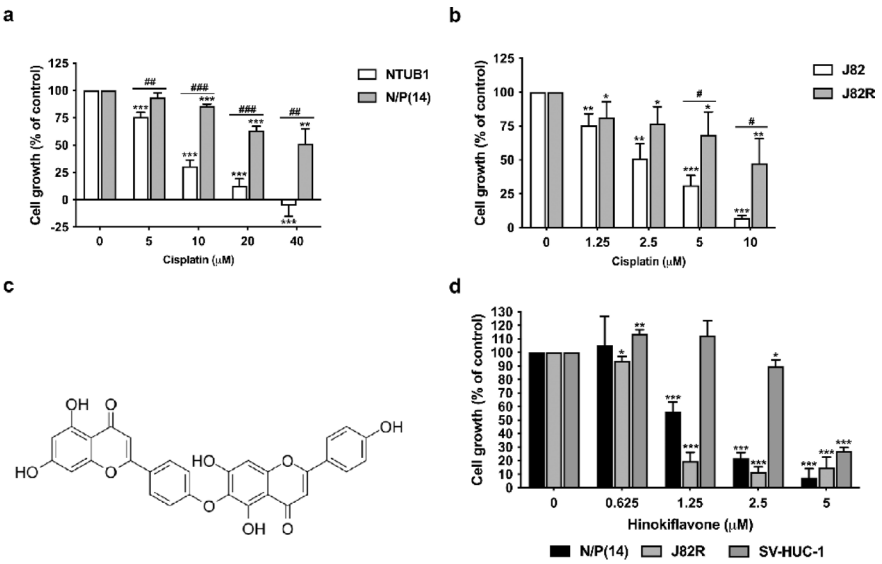

Fig. 1. Hinokiflavone exhibits differential anti-proliferative activity in cisplatin-resistant BC cell lines. (**a**–**b**) Characterization of cisplatin resistance in BC cell lines. NTUB1 and J82 cells, along with their corresponding cisplatin-resistant sublines, N/P(14) and J82R, were treated with cisplatin for 48 h and analyzed using the SRB assay. (**c**) Chemical structure of hinokiflavone. (**d**) Hinokiflavone exhibits selective anti-proliferative activity in cisplatin-resistant N/P(14) and J82R cells compared to normal uroepithelial SV-HUC-1 cells following 48 h of treatment. Data are presented as mean ± SD. ($n = 3$). Statistical analyses were performed by unpaired two-tailed Student's *t*-test. * $p < 0.05$, ** $p < 0.01$, *** $p < 0.001$ compared to control group; $^{\#}p < 0.05$, $^{\#\#}p < 0.01$, $^{\#\#\#}p < 0.001$ compared to NTUB1 or J82 group.

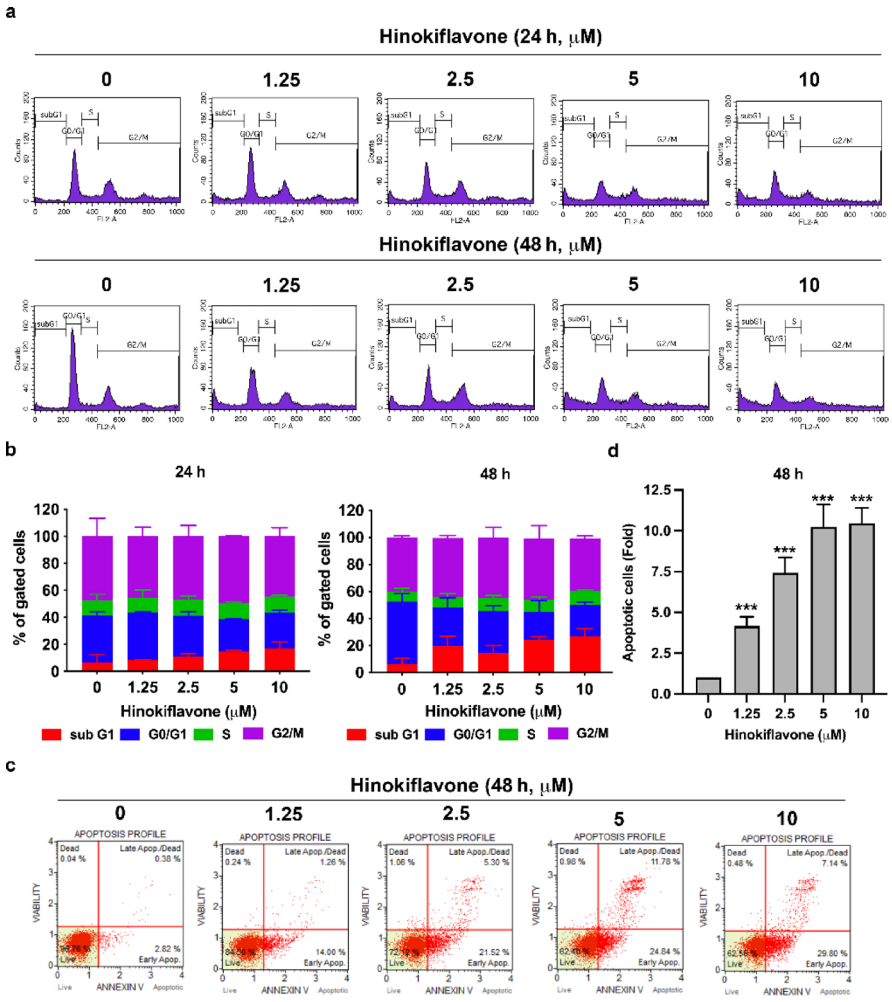

Fig. 2. Hinokiflavone promotes cell cycle accumulation at the sub-G1 phase and induces apoptosis in N/P(14) cells. (**a**) N/P(14) cells were treated with different concentrations of hinokiflavone for 24–48 h. Cell cycle distribution was analyzed by propidium iodide staining and flow cytometry. (**b**) Quantitative data of histograms are expressed as mean±S.D. ($n = 2$). (**c**) N/P(14) cells were treated with varying concentrations of hinokiflavone for 48 h, stained with Annexin V/7-AAD, and analyzed via flow cytometry. (**d**). Quantification of apoptotic cells (early- and late-stage) are expressed as mean±S.D. ($n = 3$). Statistical analyses were performed by unpaired two-tailed Student's *t*-test. ***$p < 0.001$ compared with the control group.

HNK (5 μM) for 24 h, after which total RNA was extracted and subjected to NGS analysis. Gene set enrichment analysis (GSEA) was conducted to identify affected pathways. The results indicated that HNK modulates genes involved in biosynthesis, metabolism, DNA replication, and DNA repair (Fig. 4a). Since cisplatin induces DNA lesions, which are critical for triggering the DNA damage response and mitochondrial apoptosis[13], enhanced DNA damage detection, manipulation, and repair mechanisms contribute to cisplatin resistance[14]. Notably, GSEA revealed that HNK downregulated the expression of genes associated with base excision repair (BER) in N/P(14) cells (Fig. 4b and c). To validate these findings, RT-qPCR and Western blot analyses were performed, and the results confirmed that HNK reduced the mRNA and protein levels of MUTYH, OGG1, and XRCC1 in N/P(14) cells (Fig. 4d and g). Collectively, these findings demonstrate that HNK downregulates the expression of BER-related genes in N/P(14) cells, potentially impairing the DNA repair capacity associated with cisplatin resistance.

HNK is a novel CK2 inhibitor that suppresses survival and DNA-repair pathways

Recent studies have shown that natural flavones and flavonols with a planar structure and at least two hydroxyl groups at positions 7 and 4', such as apigenin, luteolin kaempferol, fisetin, quercetin, and myricetin[43,44], exhibit inhibitory activity against CK2. HNK is a C–O–C-type biflavonoid composed of two apigenin units connected by an ether linkage[21]. On the basis of this structural similarity, we hypothesized that HNK may also inhibit CK2 activity in cisplatin-resistant BC cells. An in vitro kinase assay confirmed that HNK inhibited CK2α activity in a concentration-dependent manner (Fig. 5a). This finding was validated by Western blot analysis, the results of which demonstrated that HNK suppressed the phosphorylation of the CK2 substrate consensus sequence ((pS/pT)DXE)[45] in a concentration-dependent manner after 24 h and 48 h in N/P(14) cells (Fig. 5b), implying the

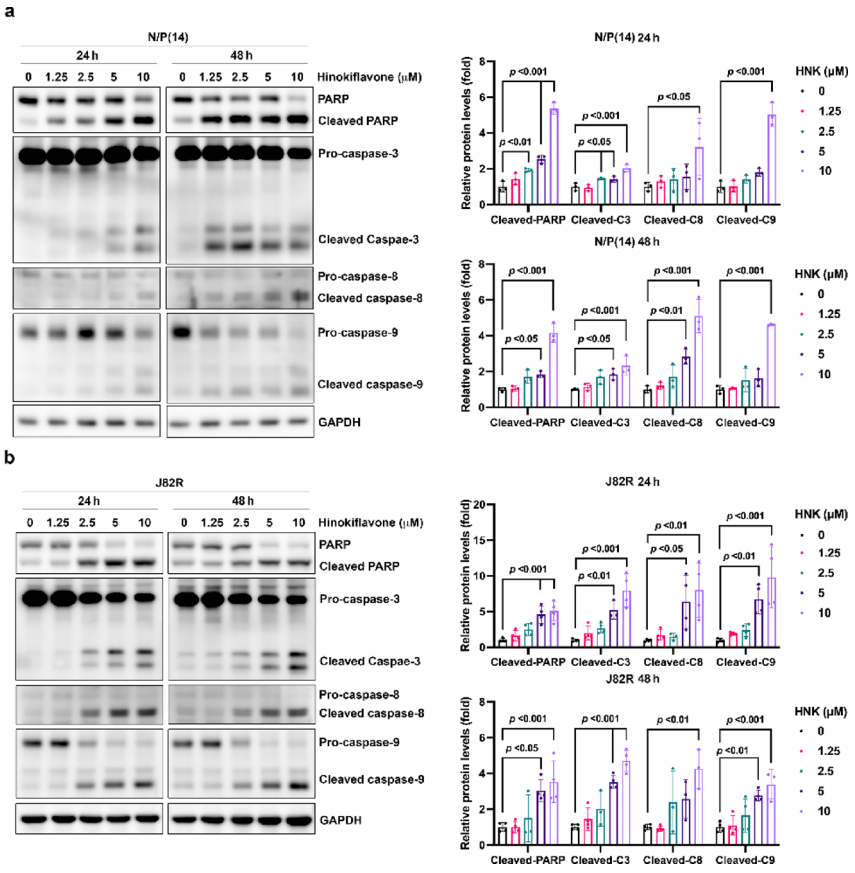

Fig. 3. Hinokiflavone increases caspase-dependent apoptosis in cisplatin-resistant BC cells. (**a**–**b**) N/P(14) (**a**) and J82R (**b**) cells were treated with the indicated concentrations of hinokiflavone (HNK) for 24–48 h, and the expression of apoptotic proteins were analyzed by western blot. The band intensities of each protein were quantified using ImageJ software and normalized to that of GAPDH. Fold changes compared to the control (0) group are expressed as the mean±S.D. ($n = 3–4$). One-way ANOVA with Dunnett's multiple comparison was used to evaluate statistical significance.

inhibition of CK2 activity. We docked HNK into the binding site of CK2α to better understand their interactions. The docking results showed that HNK fits well within the binding site, with a docking score of − 10.04. HNK occupied the binding site with its two flavonoid units in distinct regions (Fig. 5c). One flavonoid unit (flavonoid A) was positioned in the hinge region of the binding site. The central ring system of flavonoid A formed two hydrogen bonds with the hinge residue V116. The hydroxyl group on the phenyl ring formed a hydrogen bond with residue K68, which plays a key role in ligand binding[46]. In addition, flavonoid A had hydrophobic interactions with surrounding residues, including L45, V53, V66, M163, and I174. The other unit (flavonoid B) was situated near the entrance of the binding site, where it formed additional interactions with nearby residues. A hydrogen bond was formed between flavonoid B and residue N117 through its ketone oxygen. Flavonoid B also formed hydrophobic interactions with residues L45 and H115. These interactions may account for the inhibitory activity of HNK against CK2α. CK2 is known to phosphorylate Akt at Ser129, increasing its stability through association with the HSP90 chaperone[47,48]. Additionally, the CK2-mediated phosphorylation of Stat3 leads to its constitutive activation[49]. Furthermore, the CK2-dependent phosphorylation of XRCC1 is essential for its stability and function in DNA repair[50]. Our data show that HNK reduced the phosphorylation of Akt (S129) and Stat3 (Y705), as well as both total and phosphorylated XRCC1, in a time- and concentration-dependent manner in N/P(14) cells (Fig. 5d and f). A similar effect was observed in J82R cells following HNK treatment for 24 h (Supplementary Figs. S1c and 1d). Collectively, these findings indicate that HNK is a novel CK2 inhibitor that suppresses the phosphorylation of Akt, Stat3, and XRCC1 in cisplatin-resistant BC cells.

HNK induces apoptosis partly by inhibiting the CK2α/Akt pathway

To further elucidate the temporal relationship between CK2α inhibition by HNK and the downstream phosphorylation of apoptosis-related proteins in cisplatin-resistant BC cells, we performed a time-course study to analyze the dynamic changes from 6 to 48 h posttreatment. The results showed that HNK suppressed the phosphorylation of Akt (Ser 129) beginning at 12 h, which coincided with PARP cleavage, whereas a reduction in XRCC phosphorylation was not observed until 18 h posttreatment (Fig. 6a). To confirm the role of CK2α inhibition in the induction of apoptosis, we treated N/P(14) cells with the well-characterized CK2α inhibitor CX-4945[51]. CX-4945 decreased the phosphorylation of the downstream targets Akt and XRCC1 in a concentration-

a

NAME	ES	NES	NOM p-val	FDR q-val	FWER p-val
KEGG_TERPENOID_BACKBONE_BIOSYNTHESIS	-0.8111175	-1.4993265	0.046683007	0.11996048	0.623
KEGG_NICOTINATE_AND_NICOTINAMIDE_METABOLISM	-0.80109435	-1.6398011	0.005076172	0.09653887	0.193
KEGG_BASE_EXCISION_REPAIR	-0.77957356	-1.7581879	0.002475248	0.07642543	0.043
KEGG_HOMOLOGOUS_RECOMBINATION	-0.76121306	-1.5784544	0.011600928	0.09274515	0.334
KEGG_GLYCOSYLPHOSPHATIDYLINOSITOL_GPI_ANCHOR_BIOSYNTHESIS	-0.7558796	-1.572133	0.010498688	0.08817683	0.354
KEGG_AMINOACYL_TRNA_BIOSYNTHESIS	-0.73411435	-1.4955713	0.02891566	0.11547855	0.635
KEGG_VALINE_LEUCINE_AND_ISOLEUCINE_DEGRADATION	-0.69724417	-1.606846	0.00729927	0.093853116	0.269
KEGG_FATTY_ACID_METABOLISM	-0.6860208	-1.5868322	0.005050505	0.10073916	0.321
KEGG_PEROXISOME	-0.67507151	-1.7311914	0	0.052763406	0.057
KEGG_DNA_REPLICATION	-0.66752553	-1.5015891	0.019417476	0.12543479	0.613

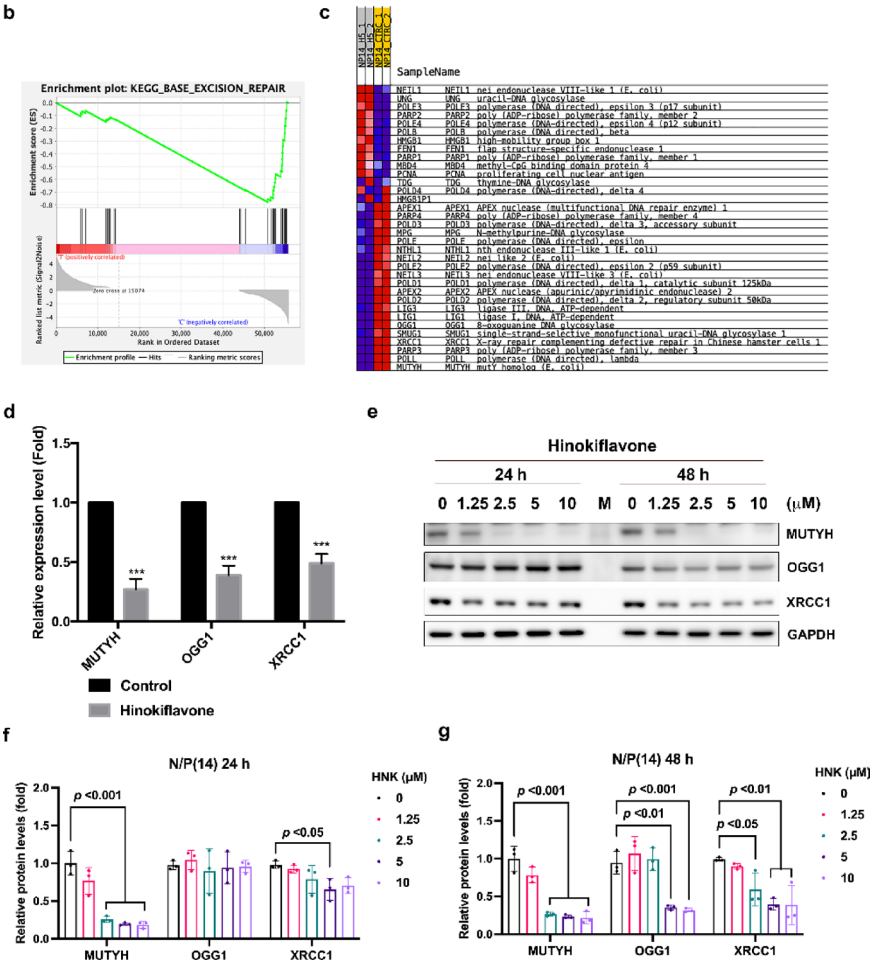

Fig. 4. Effect of hinokiflavone on the transcriptome of N/P(14) cells. The cells were treated with hinokiflavone (5 μM) for 24 h. Total RNA was extracted using TRIzol reagent and subjected to next-generation sequencing (NGS) and bioinformatics analyses ($n = 2$). The gene set enrichment analysis was performed by using the GSEA software (version 4.0.3) (https://www.gsea-msigdb.org/gsea/index.jsp). The top 10 KEGG pathways displaying the most significant enrichment in differentially expressed genes were shown (**a**), and the base excision repair (BER) pathway is significantly enriched (**b**–**c**). (**d**) Effects of hinokiflavone on BER-related genes in N/P(14) cells. Cells were treated with hinokiflavone (5 μM) for 24 h and mRNA levels determined via RT-qPCR. Data are expressed as mean±S.D ($n = 3$). Statistical analyses were performed by unpaired two-tailed Student's *t*-test. ***$p < 0.001$ compared with control group. (**e**–**g**) The effects of hinokiflavone (HNK) on the levels of BER-related proteins in N/P(14) cells were analyzed by western blotting. The band intensities of each protein were quantified using ImageJ software and normalized to that of GAPDH. Fold changes compared to the control (0) group are expressed as the mean±S.D. ($n = 3$). One-way ANOVA with Dunnett's multiple comparison was used to evaluate statistical significance.

dependent manner and increased PARP cleavage, indicating the induction of apoptosis (Fig. 6b). Furthermore, the ectopic expression of CK2α partially reversed the HNK-mediated suppression of Akt phosphorylation and PARP cleavage, highlighting the contribution of CK2α inhibition to HNK-induced apoptosis (Fig. 6c and d). The overexpression of constitutively active myristoylated Akt (Myr-Akt) also attenuated HNK-induced PARP cleavage (Figs. 6e, and 6f). Collectively, these findings suggest that HNK induces apoptosis, in part, through the inhibition of the CK2α/Akt signaling in cisplatin-resistant BC cells.

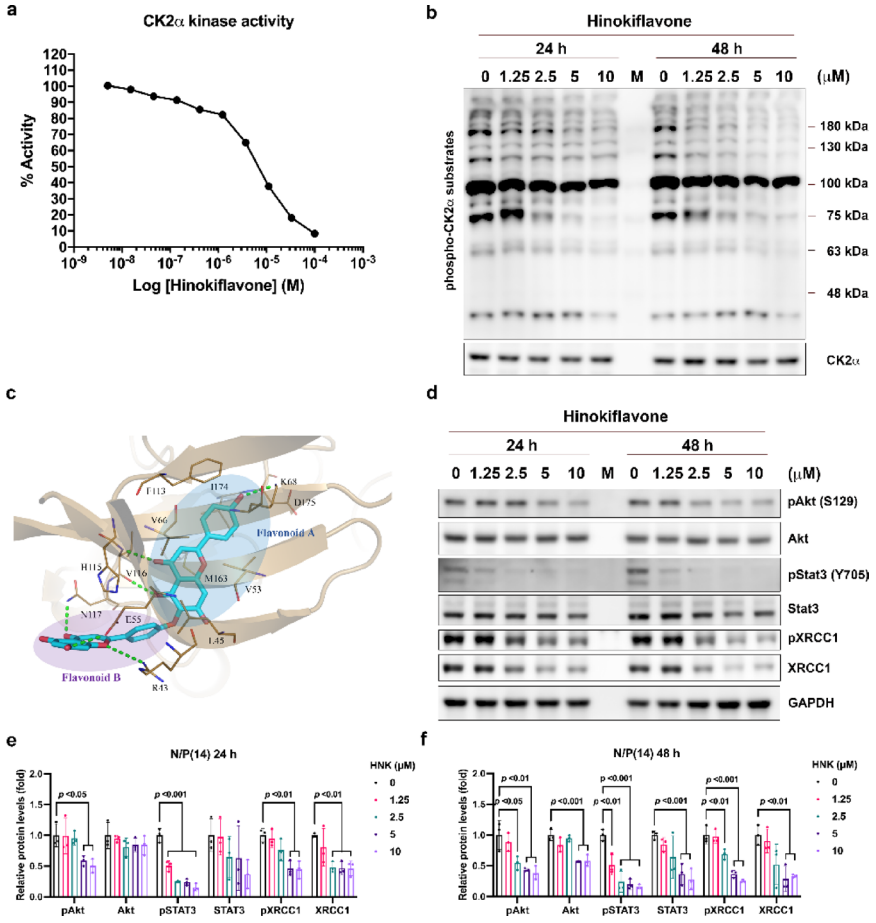

Fig. 5. Hinokiflavone is a novel CK2 inhibitor. (**a**) The in vitro inhibitory activity of hinokiflavone against CK2α was assessed by using the service of Reaction Biology Corp. The compound was tested in a 10-dose IC_{50} mode with a 3-fold serial dilution starting at 100 μM in the presence of 10 μM ATP. Data are represented as the percentage of kinase activity relative to the control group. (**b**) Effect of hinokiflavone on the phosphorylation of CK2 substrates in N/P(14) cells. Cells were treated with hinokiflavone for 24–48 h and analyzed by western blot using an antibody against the consensus sequence of CK2 substrates ((pS/pT)DXE). (**c**) Docking pose of hinokiflavone in the binding site of CK2α. Hinokiflavone is composed of two flavonoid units, labeled as flavonoid A and flavonoid B. Hydrogen bonds are shown as green dashed lines (**d–f**) N/P(14) cells were exposed to various concentrations of hinokiflavone (HNK) for 24–48 h and subjected to western blot analysis by using indicated antibodies. M: protein marker. The band intensities of each protein were quantified using ImageJ software and normalized to that of GAPDH. Fold changes compared to the control (0) group are expressed as the mean±S.D. ($n = 3$). One-way ANOVA with Dunnett's multiple comparison was used to evaluate statistical significance.

Synergistic interaction between HNK and chemotherapeutic agents in cisplatin-resistant BC cells

The above mentioned data suggest that HNK downregulates the expression of genes associated with base excision repair (BER) in N/P(14) cells (Figs. 4, and 5). On this basis, we hypothesized that HNK may increase the efficacy of chemotherapeutic agents in BC. Doxorubicin and mitomycin C are commonly used for the intravesical instillation in NMIBC patients[2]. Our results demonstrated that HNK synergistically enhances the therapeutic effects of doxorubicin and mitomycin C in N/P(14) cells, as indicated by combination index (CI) values below 1 (Fig. 7a and b). Additionally, the combination of HNK with doxorubicin or mitomycin C further increased apoptosis in N/P(14) cells, as evidenced by the increased cleavage of caspase-3 and PARP (Fig. 6c). These findings highlight the potential role of HNK as a chemosensitizing agent.

Discussion

Platinum-based chemotherapies, including MVAC, ddMVAC, and GC, constitute the standard of care for patients with advanced BC[6]. However, the median survival of BC patients who experience relapse after platinum-based chemotherapy is only 5–7 months[12]. Therefore, developing chemosensitizing strategies remains an urgent clinical need. In this study, we identified hinokiflavone (HNK), a biflavonoid, as a potential therapeutic agent that inhibits the growth of cisplatin-resistant BC cells while sparing normal uroepithelial cells (Fig. 1).

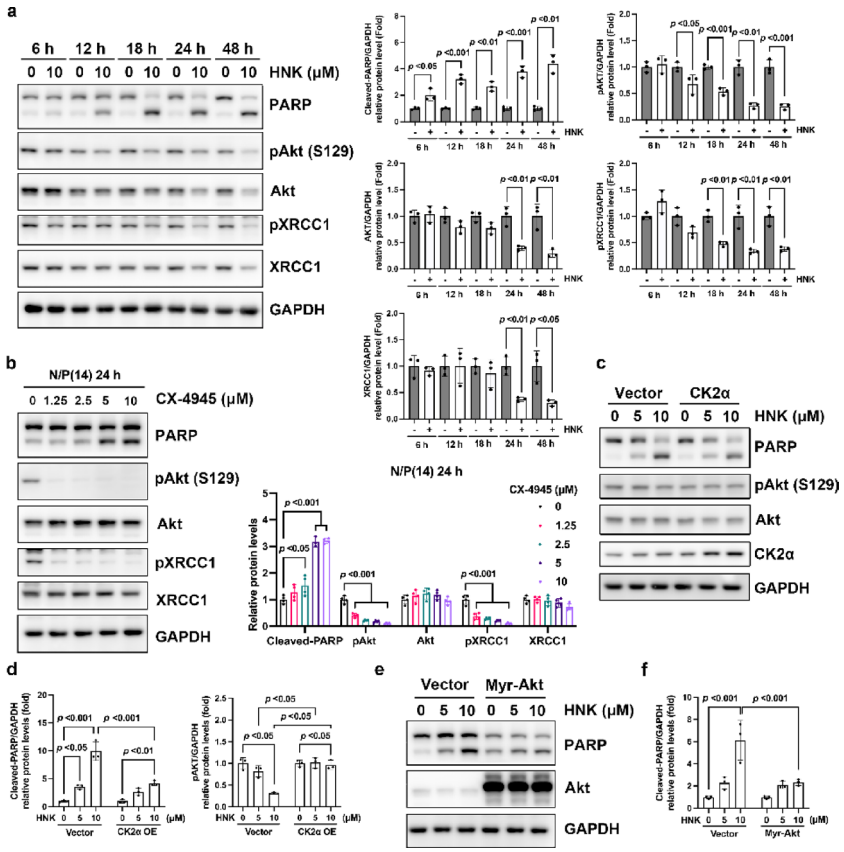

Fig. 6. Hinokiflavone induces apoptosis partially through inhibition of the CK2α/Akt signaling in N/P(14) cells. (**a**) N/P(14) cells were treated with hinokiflavone (HNK, 10 μM) for the indicated times (6–48 h), followed by Western blot analysis by indicated antibodies. (**b**) N/P(14) cells were treated with increasing concentrations of CX-4945 for 24 h, and subjected to Western blotting by indicated antibodies. (**c–d**) N/P(14) cells were transfected with vector control or CK2α-expressing plasmid for 24 h, followed by treatment with HNK for another 24 h, and subjected to Western blotting. (**e–f**) N/P(14) cells were transfected with vector control or constitutively active myristoylated Akt (Myr-Akt) for 24 h, followed by HNK treatment for an additional 24 h, and subjected to Western blotting. The band intensities of each protein were quantified using ImageJ software and normalized to that of GAPDH. Data are expressed as the mean±S.D. ($n = 3$). Statistical analyses were performed by unpaired two-tailed Student's *t*-test in **a**; one-way ANOVA with Dunnett's multiple comparison in **b**; two-way ANOVA with Tukey's multiple comparison in **c** and **e**.

Mechanistically, HNK transcriptionally suppressed genes associated with base excision repair (Fig. 4) and induced apoptosis in cisplatin-resistant BC cells (Figs. 2 and 3). Notably, our study is the first to reveal that HNK functions as a novel CK2 inhibitor, abrogating the phosphorylation of Akt, Stat3, and XRCC1 (Fig. 5). Moreover, HNK synergistically enhanced the therapeutic efficacy of doxorubicin and mitomycin C in N/P(14) cells (Fig. 7). Collectively, these findings indicate that HNK, by targeting both DNA repair pathways and CK2-mediated survival signaling, is a promising therapeutic candidate for cisplatin-resistant BC.

HNK is a biflavonoid composed of two apigenin units connected via a C–O–C ether linkage[21]; it was first isolated from *Chamaecyparis obtusa* Endlicher in Japan but has also been identified in various plant species within the *Cupressaceae* and *Taxaceae* families[22]. Previous studies have highlighted the diverse pharmacological properties of HNK, including anti-inflammatory, antioxidant, and antitumor activities[26–29]. In addition to its potent antiproliferative and antimigratory effects, HNK has demonstrated significant antitumor activity, particularly in breast cancer, colon cancer, and hepatocellular carcinoma (HCC) models[29–31]. Additionally, HNK can be synthetically produced, and its oral micellar formulation has been reported to enhance its proapoptotic and anticancer effects both in vitro and in vivo[23,52], further demonstrating its potential as a clinical therapeutic agent. However, the molecular target of HNK and the pharmacological mechanism underlying its anticancer activity remain elusive. In this study, we provide evidence that HNK functions as a novel inhibitor of CK2α. This result expands upon previous findings that certain natural flavones and flavonols, such as apigenin, luteolin, and quercetin, can inhibit CK2 activity due to their planar structure and hydroxyl substitutions at specific positions[43,44]. Given that HNK consists of two apigenin units, we hypothesized that its unique biflavonoid structure may enhance its interaction with CK2. Molecular docking analysis revealed that the two flavonoid moieties of HNK occupy distinct regions of the CK2α binding pocket and establish multiple stabilizing interactions (Fig. 5c). Specifically, one moiety binds in the hinge region via hydrogen bonds with V116 and

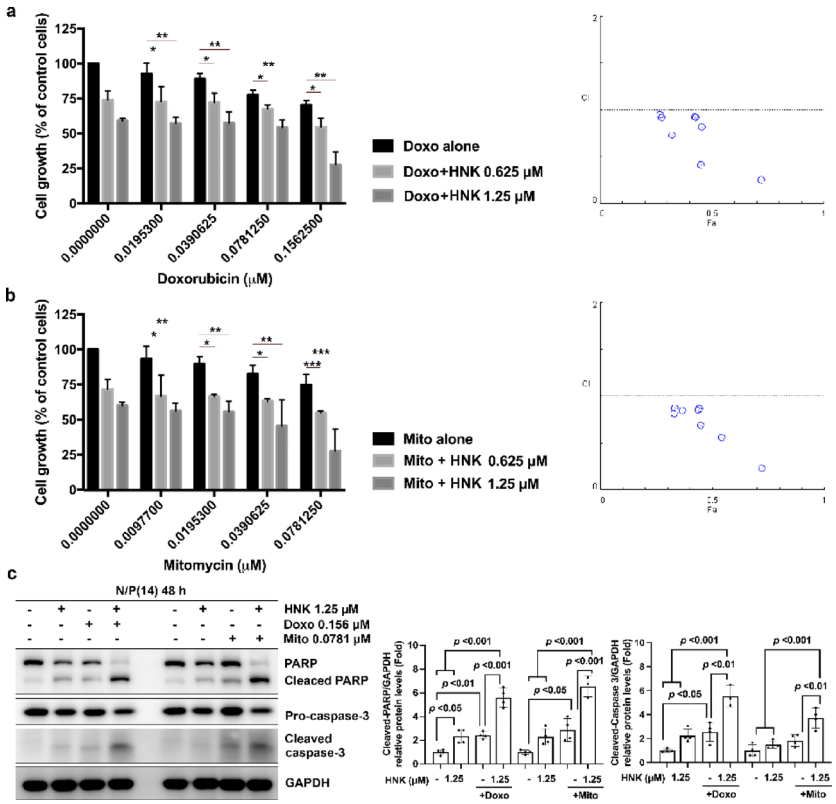

Fig. 7. Synergistic interaction between hinokiflavone and chemotherapeutic agents in N/P(14) cells. (**a**–**b**) The cells were treated with doxorubicin (**a**, doxo) or mitomycin C (**b**, mito) in the presence or absence of hinokiflavone (HNK) for 48 h, and subjected to SRB assay. The combination index (CI) values were calculated and plotted by CompuSyn software. (**c**) N/P(14) cells were exposed to indicated compounds for 48 h, and the protein expression of apoptotic proteins were analyzed by western blot. The band intensities of each protein were quantified using ImageJ software and normalized to that of GAPDH. Data are expressed as the mean±S.D. ($n = 3$–4). Statistical analyses were performed by two-way ANOVA with Tukey's multiple comparison.

K68, along with hydrophobic contacts with several adjacent residues. The second moiety extends toward the pocket entrance, forming additional hydrogen and hydrophobic interactions. These multivalent contacts likely contribute to the inhibitory activity of HNK against CK2α.

HNK has been reported to function as an inhibitor of SUMO/Sentrin-specific protease 1 (SENP1), leading to the accumulation of SUMOylated proteins[53]. Moreover, the inhibition of matrix metalloproteases (MMPs) represents another key mechanism of HNK, contributing to its antiangiogenic and antimetastatic effects in cancer[54]. For the first time, we identified HNK as a novel casein kinase 2 (CK2) inhibitor, as evidenced by its suppression of CK2 kinase activity and the subsequent decrease in the phosphorylation of CK2 substrates, including Akt, Stat3, and XRCC1 (Fig. 5). Specifically, CK2 phosphorylates XRCC1, a key scaffold protein in the base excision repair (BER) and single-strand break repair (SSBR) pathways, stabilizing the XRCC1–DNA ligase IIIa complex[50]. Our data demonstrated a synergistic interaction between HNK and DNA-damaging chemotherapeutic agents, such as doxorubicin and mitomycin C, enhancing their therapeutic efficacy (Fig. 7). Notably, CK2-specific inhibitors have been reported to reverse cisplatin resistance in non-small cell lung cancer[55,56]. Given that increased DNA repair capacity is a major contributor to cisplatin resistance[14], our findings suggest a potential strategy to overcome such resistance by targeting CK2-mediated XRCC1 stabilization and function in cisplatin-resistant BC cells.

In conclusion, our study identified HNK as a promising therapeutic candidate for overcoming cisplatin resistance in BC. This is the first study to demonstrate that HNK functions as a novel CK2 inhibitor, selectively inhibiting the proliferation of cisplatin-resistant BC cells while sparing normal uroepithelial cells. Mechanistically, HNK suppresses the expression of genes involved in base excision repair and induces apoptosis. Furthermore, HNK synergistically enhances the efficacy of chemotherapeutic agents such as doxorubicin and mitomycin C, underscoring its potential as a chemosensitizing agent. These findings provide strong evidence supporting HNK as a therapeutic strategy to improve treatment outcomes for patients with cisplatin-resistant BC.

Data availability

The datasets generated and analyzed during the current study are available in the Gene Expression Omnibus (GEO) repository, [GSE290747]. (https://www.ncbi.nlm.nih.gov/geo/query/acc.cgi? acc=GSE290747)

Received: 22 February 2025; Accepted: 9 June 2025
Published online: 01 July 2025

References

1. Bray, F. et al. Global cancer statistics 2022: GLOBOCAN estimates of incidence and mortality worldwide for 36 cancers in 185 countries. *CA Cancer J. Clin.* **74**, 229–263. https://doi.org/10.3322/caac.21834 (2024).
2. Lenis, A. T., Lec, P. M., Chamie, K. & Mshs, M. D. Bladder cancer: A review. *JAMA* **324**, 1980–1991. https://doi.org/10.1001/jama.2020.17598 (2020).
3. Babjuk, M. et al. EAU guidelines on non-muscle-invasive urothelial carcinoma of the bladder: update 2013. *Eur. Urol.* **64**, 639–653. https://doi.org/10.1016/j.eururo.2013.06.003 (2013).
4. Funt, S. A. & Rosenberg, J. E. Systemic, perioperative management of muscle-invasive bladder cancer and future horizons. *Nat. Rev. Clin. Oncol.* **14**, 221–234. https://doi.org/10.1038/nrclinonc.2016.188 (2017).
5. Ghosh, M., Brancato, S. J., Agarwal, P. K. & Apolo, A. B. Targeted therapies in urothelial carcinoma. *Curr. Opin. Oncol.* **26**, 305–320. https://doi.org/10.1097/CCO.0000000000000064 (2014).
6. Bukhari, N., Al-Shamsi, H. O. & Azam, F. Update on the treatment of metastatic urothelial carcinoma. *ScientificWorldJournal* **2018**, 5682078. https://doi.org/10.1155/2018/5682078 (2018).
7. Labadie, B. W., Balar, A. V. & Luke, J. J. Immune checkpoint inhibitors for genitourinary cancers: treatment indications, investigational approaches and biomarkers. *Cancers (Basel)*. 13. https://doi.org/10.3390/cancers13215415 (2021).
8. Afonso, J., Santos, L. L., Longatto-Filho, A. & Baltazar, F. Competitive glucose metabolism as a target to boost bladder cancer immunotherapy. *Nat. Rev. Urol.* **17**, 77–106. https://doi.org/10.1038/s41585-019-0263-6 (2020).
9. Scholtes, M. et al. Targeted therapy in metastatic bladder cancer: present status and future directions. *Appl. Sci.* **10**, 7102 (2020).
10. Powles, T. et al. Enfortumab Vedotin and pembrolizumab in untreated advanced urothelial Cancer. *N Engl. J. Med.* **390**, 875–888. https://doi.org/10.1056/NEJMoa2312117 (2024).
11. Hoimes, C. J. et al. A plain Language summary exploring a new treatment combination for untreated locally advanced or metastatic urothelial cancer: enfortumab Vedotin plus pembrolizumab. *Future Oncol.* **20**, 351–360. https://doi.org/10.2217/fon-2023-0112 (2024).
12. Flaig, T. W. et al. NCCN guidelines insights: bladder cancer, version 5.2018. *J. Natl. Compr. Canc Netw.* **16**, 1041–1053. https://doi.org/10.6004/jnccn.2018.0072 (2018).
13. Galluzzi, L. et al. Molecular mechanisms of cisplatin resistance. *Oncogene* **31**, 1869–1883. https://doi.org/10.1038/onc.2011.384 (2012).
14. Drayton, R. M. & Catto, J. W. Molecular mechanisms of cisplatin resistance in bladder cancer. *Expert Rev. Anticancer Ther.* **12**, 271–281. https://doi.org/10.1586/era.11.201 (2012).
15. Newman, D. J. & Cragg, G. M. Natural products as sources of new drugs over the 30 years from 1981 to 2010. *J. Nat. Prod.* **75**, 311–335. https://doi.org/10.1021/np200906s (2012).
16. Newman, D. J. & Cragg, G. M. Natural products as sources of new drugs over the nearly four decades from 01/1981 to 09/2019. *J. Nat. Prod.* **83**, 770–803. https://doi.org/10.1021/acs.jnatprod.9b01285 (2020).
17. Perez, E. A. Microtubule inhibitors: differentiating tubulin-inhibiting agents based on mechanisms of action, clinical activity, and resistance. *Mol. Cancer Ther.* **8**, 2086–2095. https://doi.org/10.1158/1535-7163.MCT-09-0366 (2009).
18. Patel, V. G., Oh, W. K. & Galsky, M. D. Treatment of muscle-invasive and advanced bladder cancer in 2020. *CA Cancer J. Clin.* **70**, 404–423. https://doi.org/10.3322/caac.21631 (2020).
19. Kopustinskiene, D. M., Jakstas, V., Savickas, A. & Bernatoniene, J. Flavonoids as Anticancer Agents. *Nutrients* 12, (2020). https://doi.org/10.3390/nu12020457
20. Panche, A. N., Diwan, A. D. & Chandra, S. R. Flavonoids: an overview. *J. Nutr. Sci.* **5**, e47. https://doi.org/10.1017/jns.2016.41 (2016).
21. Gontijo, V. S., Dos Santos, M. H. & Viegas, C. Jr. Biological and chemical aspects of natural biflavonoids from plants: A brief review. *Mini Rev. Med. Chem.* **17**, 834–862. https://doi.org/10.2174/1389557517666161104130026 (2017).
22. Goossens, J. F., Goossens, L. & Bailly, C. Hinokiflavone and related C-O-C-Type biflavonoids as Anti-cancer compounds: properties and mechanism of action. *Nat. Prod. Bioprospect.* **11**, 365–377. https://doi.org/10.1007/s13659-021-00298-w (2021).
23. Sagrera, G., Bertucci, A., Vazquez, A. & Seoane, G. Synthesis and antifungal activities of natural and synthetic biflavonoids. *Bioorg. Med. Chem.* **19**, 3060–3073. https://doi.org/10.1016/j.bmc.2011.04.010 (2011).
24. Lee, S. et al. Ameliorative effects of Juniperus rigida fruit on oxazolone- and 2,4-dinitrochlorobenzene-induced atopic dermatitis in mice. *J. Ethnopharmacol.* **214**, 160–167. https://doi.org/10.1016/j.jep.2017.12.022 (2018).
25. Zhuang, B. et al. Chemical profiling and quantitation of bioactive compounds in Platycladi cacumen by UPLC-Q-TOF-MS/MS and UPLC-DAD. *J. Pharm. Biomed. Anal.* **154**, 207–215. https://doi.org/10.1016/j.jpba.2018.03.005 (2018).
26. Wang, G., Yao, S., Zhang, X. X. & Song, H. Rapid screening and structural characterization of antioxidants from the extract of Selaginella doederleinii Hieron with DPPH-UPLC-Q-TOF/MS method. *Int. J. Anal. Chem.* **2015** (849769). https://doi.org/10.1155/2015/849769 (2015).
27. Kim, H. P., Park, H., Son, K. H., Chang, H. W. & Kang, S. S. Biochemical Pharmacology of biflavonoids: implications for anti-inflammatory action. *Arch. Pharm. Res.* **31**, 265–273. https://doi.org/10.1007/s12272-001-1151-3 (2008).
28. Shim, S. Y., Lee, S. G. & Lee, M. Biflavonoids isolated from Selaginella Tamariscina and their Anti-Inflammatory activities via ERK 1/2 signaling. *Molecules* **23** https://doi.org/10.3390/molecules23040926 (2018).
29. Zhou, J. et al. Antitumor activity in colorectal cancer induced by Hinokiflavone. *J. Gastroenterol. Hepatol.* **34**, 1571–1580. https://doi.org/10.1111/jgh.14581 (2019).
30. Huang, W. et al. Hinokiflavone induces apoptosis and inhibits migration of breast cancer cells via EMT signalling pathway. *Cell. Biochem. Funct.* **38**, 249–256. https://doi.org/10.1002/cbf.3443 (2020).
31. Lee, K. C., Chen, W. T., Liu, Y. C., Lin, S. S. & Hsu, F. T. Amentoflavone inhibits hepatocellular carcinoma progression through blockage of ERK/NF-kB activation. *Vivo* **32**, 1097–1103. https://doi.org/10.21873/invivo.11351 (2018).
32. Chen, C. H. et al. Dual Inhibition of PIK3C3 and FGFR as a new therapeutic approach to treat bladder Cancer. *Clin. Cancer Res.* **24**, 1176–1189. https://doi.org/10.1158/1078-0432.CCR-17-2066 (2018).
33. Huang, C. Y. et al. Ling-Zhi polysaccharides potentiate cytotoxic effects of anticancer drugs against drug-resistant urothelial carcinoma cells. *J. Agric. Food Chem.* **58**, 8798–8805. https://doi.org/10.1021/jf1020158 (2010).
34. Chen, M. C., Lin, Y. C., Liao, Y. H., Liou, J. P. & Chen, C. H. MPT0G612, a novel HDAC6 inhibitor, induces apoptosis and suppresses IFN-gamma-Induced programmed Death-Ligand 1 in human colorectal carcinoma cells. *Cancers (Basel).* **11** https://doi.org/10.3390/cancers11101617 (2019).
35. Tu, C. C. et al. Targeting PPARgamma via SIAH1/2-mediated ubiquitin-proteasomal degradation as a new therapeutic approach in luminal-type bladder cancer. *Cell. Death Dis.* **15**, 908. https://doi.org/10.1038/s41419-024-07298-x (2024).
36. Chang, C. H. et al. Stellettin B Induces Cell Death in Bladder Cancer Via Activating the Autophagy/DAPK2/Apoptosis Signaling Cascade. *Mar Drugs* 21, (2023). https://doi.org/10.3390/md21020073
37. Subramanian, A. et al. Gene set enrichment analysis: a knowledge-based approach for interpreting genome-wide expression profiles. *Proc. Natl. Acad. Sci. U S A.* **102**, 15545–15550. https://doi.org/10.1073/pnas.0506580102 (2005).

38. Mootha, V. K. et al. PGC-1alpha-responsive genes involved in oxidative phosphorylation are coordinately downregulated in human diabetes. *Nat. Genet.* **34**, 267–273. https://doi.org/10.1038/ng1180 (2003).
39. Schrödinger Release 2022-3. Maestro, Schrödinger, LLC, New York, NY, (2021).
40. Berman, H. M. et al. The protein data bank. *Nucleic Acids Res.* **28**, 235–242. https://doi.org/10.1093/nar/28.1.235 (2000).
41. Friesner, R. A. et al. Glide: A new approach for rapid, accurate Docking and scoring. 1. Method and assessment of Docking accuracy. *J. Med. Chem.* **47**, 1739–1749. https://doi.org/10.1021/jm0306430 (2004).
42. Biovia, D. S. Pipeline Pilot. *Dassault Systèmes* (2021).
43. Lolli, G. et al. Inhibition of protein kinase CK2 by flavonoids and tyrphostins. A structural insight. *Biochemistry* **51**, 6097–6107. https://doi.org/10.1021/bi300531c (2012).
44. McCarty, M. F., Assanga, S. I. & Lujan, L. L. Flavones and flavonols May have clinical potential as CK2 inhibitors in cancer therapy. *Med. Hypotheses*. **141**, 109723. https://doi.org/10.1016/j.mehy.2020.109723 (2020).
45. Meggio, F. & Pinna, L. A. One-thousand-and-one substrates of protein kinase CK2? *FASEB J.* **17**, 349–368. https://doi.org/10.1096/fj.02-0473rev (2003).
46. Battistutta, R. et al. The ATP-binding site of protein kinase CK2 holds a positive electrostatic area and conserved water molecules. *ChemBioChem* **8**, 1804–1809. https://doi.org/10.1002/cbic.200700307 (2007).
47. Di Maira, G. et al. Protein kinase CK2 phosphorylates and upregulates akt/pkb. *Cell. Death Differ.* **12**, 668–677. https://doi.org/10.1038/sj.cdd.4401604 (2005).
48. Di Maira, G., Brustolon, F., Pinna, L. A. & Ruzzene, M. Dephosphorylation and inactivation of akt/pkb is counteracted by protein kinase CK2 in HEK 293T cells. *Cell. Mol. Life Sci.* **66**, 3363–3373. https://doi.org/10.1007/s00018-009-0108-1 (2009).
49. Rozovski, U. et al. Constitutive phosphorylation of STAT3 by the CK2-BLNK-CD5 complex. *Mol. Cancer Res.* **15**, 610–618. https://doi.org/10.1158/1541-7786.MCR-16-0291 (2017).
50. Parsons, J. L. et al. XRCC1 phosphorylation by CK2 is required for its stability and efficient DNA repair. *DNA Repair. (Amst).* **9**, 835–841. https://doi.org/10.1016/j.dnarep.2010.04.008 (2010).
51. Siddiqui-Jain, A. et al. CX-4945, an orally bioavailable selective inhibitor of protein kinase CK2, inhibits prosurvival and angiogenic signaling and exhibits antitumor efficacy. *Cancer Res.* **70**, 10288–10298. https://doi.org/10.1158/0008-5472.CAN-10-1893 (2010).
52. Chen, Y., Feng, X., Li, L., Song, K. & Zhang, L. Preparation and antitumor evaluation of Hinokiflavone hybrid micelles with mitochondria targeted for lung adenocarcinoma treatment. *Drug Deliv.* **27**, 565–574. https://doi.org/10.1080/10717544.2020.1748760 (2020).
53. Pawellek, A. et al. Characterisation of the biflavonoid Hinokiflavone as a pre-mRNA splicing modulator that inhibits SENP. *Elife* **6** https://doi.org/10.7554/eLife.27402 (2017).
54. Menezes, J. & Diederich, M. F. Bioactivity of natural biflavonoids in metabolism-related disease and cancer therapies. *Pharmacol. Res.* **167**, 105525. https://doi.org/10.1016/j.phrs.2021.105525 (2021).
55. Wang, Y., Wang, X., Xu, G. & Gou, S. Novel CK2-Specific Pt(II) compound reverses Cisplatin-Induced resistance by inhibiting Cancer cell stemness and suppressing DNA damage repair in Non-small cell lung Cancer treatments. *J. Med. Chem.* **64**, 4163–4178. https://doi.org/10.1021/acs.jmedchem.1c00079 (2021).
56. Jin, C., Song, P. & Pang, J. The CK2 inhibitor CX4945 reverses cisplatin resistance in the A549/DDP human lung adenocarcinoma cell line. *Oncol. Lett.* **18**, 3845–3856. https://doi.org/10.3892/ol.2019.10696 (2019).

Author contributions

Conceptualization and study design: T.-H.H., H.-P.K. and C.-H.C.; data acquisition: T.-H.H., Y.-C.L., B.-J.L. and K.-C.H.; data analysis and interpretation: T.-H.H., M.-C.C., Y.-C.L., B.-J.L. and K.-C.H.; Writing - original draft preparation: T.-H.H., M.-C.C. and C.-H.C; Writing - review and editing: T.-H.H., H.-P.K., M.-C.C. and C.-H.C. Funding acquisition: H.-P.K., M.-C.C. and C.-H.C. Supervision: C.-H.C. All authors have read and agreed to the published version of the manuscript.

Funding

This study was supported by the National Science and Technology Council of Taiwan (NSTC 108-2320-B-038-027-MY3, NSTC 110-2320-B-038-033-MY3, and NSTC111-2320-B-038-032-MY3), and Taipei Medical University Hospital (111TMU-TMUH-02-1).

Declarations

Competing interests

The authors declare no competing interests.

Consent for publication

All Authors gave their consent to submit and publish the article.

Additional information

Supplementary Information The online version contains supplementary material available at https://doi.org/10.1038/s41598-025-06543-3.

Correspondence and requests for materials should be addressed to C.-H.C.